Article

# Study of the Conformational Dynamics of Prolyl Oligopeptidase by Mass Spectrometry: Lessons Learned

Roos Van Elzen, Albert Konijnenberg, Pieter Van der Veken, Matthew J. Edgeworth, James H. Scrivens, Vilmos Fülöp, Frank Sobott,* and Anne-Marie Lambeir*

Read Online

ACCESS | Metrics & More | Article Recommendations | Supporting Information

**ABSTRACT:** Ion mobility mass spectrometry (IM-MS) can be used to analyze native proteins according to their size and shape. By sampling individual molecules, it allows us to study mixtures of conformations, as long as they have different collision cross sections and maintain their native conformation after dehydration and vaporization in the mass spectrometer. Even though conformational heterogeneity of prolyl oligopeptidase has been demonstrated in solution, it is not detectable in IM-MS. Factors that affect the conformation in solution, binding of an active site ligand, the stabilizing Ser554Ala mutation, and acidification do not qualitatively affect the collision-induced unfolding pattern. However, measuring the protection of accessible cysteines upon ligand binding provides a principle for the development of MS-based ligand screening methods.
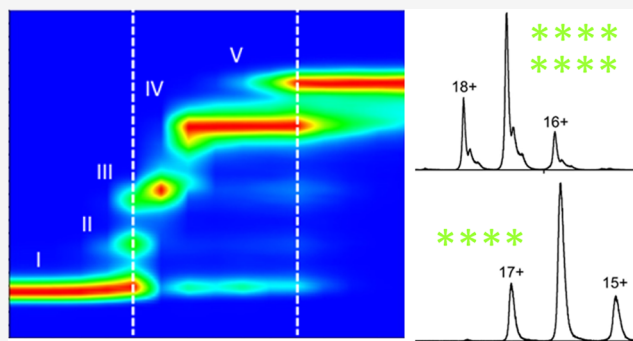
## INTRODUCTION

Recently, Pätsi et al. reported a novel class of 5-aminothiazole-containing ligands of prolyl oligopeptidase (PREP) that affect α-synuclein aggregation, reactive oxygen species (ROS) production, and autophagy irrespective of their ability to inhibit its peptidase activity.[1] Previously, Kilpeläinen et al., studying a series of 5-aminooxazoles, also reported a discrepancy between the potency of these molecules as peptidase inhibitors and their action in cell-based assays.[2] To account for this observation, it was suggested that these compounds bind in the inner cavity of PREP, remote from the substrate binding site, and somehow affect the ability of PREP to participate in the protein–protein interaction networks underlying the processes mentioned above. This opens the question of whether the novel compounds affect the conformation of the PREP protein in the same way as the potent active site inhibitors studied before. Anticipating the upcoming work on the mode of binding of these 5-aminothiazoles, maybe now is the appropriate time to share some historical observations using ion mobility native mass spectrometry (IM-MS) with recombinant porcine PREP and a covalent active site inhibitor described before (IC-13, PDB code 4BCB, structure, and potency shown in the Supporting Information, Figure S1).[3] IC-13 was first described in a structure–activity relationship, exploring the effect of P2 substituents as "pore"-binding elements. It was the most potent inhibitor of this study and also performed best in a cellular model of Parkinson's disease synucleinopathy.[3] That makes it a

relevant study object since the binding site of the newly developed 5-aminothiazoles presumably is located in PREP's internal cavity.[1] Apart from an azide group on position 4 of the P2 proline, IC-13 has a 4-phenylbutanoyl group in P3 and a P1-(2S)-cyanoproline. The electrophilic carbonitrile group forms a covalent bond with the catalytic serine of PREP, which significantly increases the affinity.[3]

The experiments reported here were performed between 2011 and 2015 using the Waters Synapt G1 HDMS (Warwick University) and Synapt G2 HDMS (University of Antwerp), which have a higher resolution. Both instruments have the same general layout but differ in their specifications. At that time, it was already recognized that soft ionization methods can preserve information on native protein structures and IM-MS was becoming established as a fairly easy and cost-efficient way to probe the conformational landscape of proteins after ligand binding and to study the effect of ligands on protein stability by collision-induced unfolding (CIU).[4,5] At the same time, there was good experimental evidence that, in solution, free PREP constitutes a heterogeneous ensemble of fairly open flexible conformations, while the PREP–inhibitor complex is

## Table 1. Methods Used to Study Ligand-Induced Conformational Changes of PREP[a]

| method | parameter | free | complex | refs |
|---|---|---|---|---|
| dynamic light scattering | hydrodynamic radius | 3.77 nm | 3.24 nm | 6 |
| nuclear magnetic resonance (NMR) | chemical shift | multiple | single | 7,8 |
| small-angle X-ray scattering in solution (SAXS) | radius of gyration maximal distance | 28.50 Å 86.2 Å | 27.40 Å 81.3 Å | 7 |
| H/D-exchange MS | flexibility | flexible | protected | 10 |
| native polyacrylamide gel electrophoresis (PAGE) | migration distance | multiple bands, slow | single band, fast | 6,10 |

[a]PREP ligands that do not affect the catalytic activity obviously cannot be screened as inhibitors but require biophysical techniques to determine their potency, mode of binding, and stoichiometry.
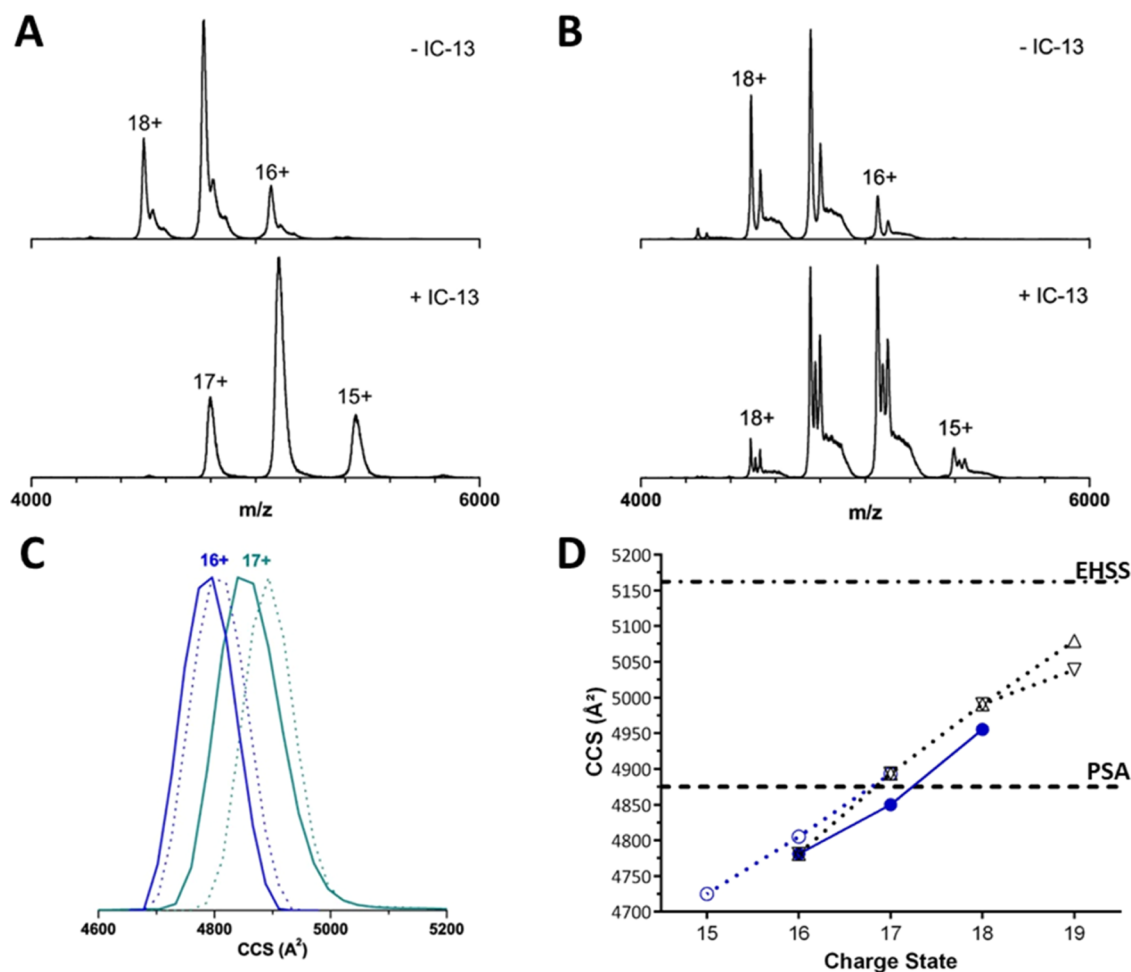


**Figure 1.** Native MS spectra and drift times. Panels (A, B) show representative native MS spectra with and without IC-13 for wtPREP and Ser554Ala, respectively. Panel (C) shows the drift profile of the +16 and +17 charge states of wtPREP in free form (solid lines) and in complex with IC-13 (dotted lines). In panel (D), the observed CCS is plotted versus the charge state of free wtPREP (blue solid circle) and the inhibitor complex (blue open circle) measured on Synapt G2. The data in black (up triangle, down triangle) are the values of free and complexed PREP obtained with the Synapt G1. Horizontal dashed and dotted lines delineate the predicted range of CCS using the EHSS and PSA programs.

homogeneous and more compact.[6−10] The different approaches and parameters used to probe the conformational dynamics of PREP are summarized in Table 1.

The hypothesis that PREP ligands cause their biological effect through protein—protein interactions independently of the peptidase activity relies, in part, on observations that the catalytically impaired PREP mutant Ser554Ala can rescue the functions lost in PREP-negative mice.[11] However, it is not known whether and how the traditional inhibitors, and indeed the new PREP ligands, bind to Ser554Ala.

To identify the binding site of their newly developed compounds, following up on results obtained by molecular modeling and dynamics, Pätsi et al. introduced point mutations

of alanine to polar side chains and cysteines to nonpolar side chains. They also describe a strategy based upon chemical modification of the introduced cysteines upon ligand binding but this experiment was not performed.[1] However, it brings to mind that such a strategy would need to work against the background of 16 free cysteines in the PREP structure.

The aim of this paper is to share previously unpublished results that may be helpful to researchers studying the conformational dynamics of PREP and the mode of binding of this new class of PREP-directed compounds. We divulge data related to three topics: (1) the suitability of native mass spectrometry to study the conformational dynamics of PREP and binding of active site ligands, (2) the stability and

conformation of the Ser554Ala mutant, and (3) the change in accessibility of cysteines upon binding of an active site inhibitor.

## ■ RESULTS AND DISCUSSION

**Native MS and IM-MS Drift Times of Free and Ligand-Bound PREP.** Native MS spectra and IM-MS drift times for free PREP and the PREP−inhibitor complex, measured with the Synapt G2, are shown in Figure 1 for both wild type and Ser554Ala. The mass spectra show a single narrow, symmetrical distribution of charge states between +19 and +15, indicative of a folded protein in a monomeric state. The differences in $m/z$ between the free and liganded proteins correspond to the theoretical mass of the inhibitor (Figures 1A,B and S3).

Note that in Figures 1B and S3, free and liganded forms of Ser554Ala coexist, consistent with the weaker binding of IC-13 to the mutant. For both proteins, inhibitor binding appears to be accompanied by a shift in charge state distribution toward lower charge states, possibly because of the loss of 1 ionization site. Drift times and corresponding collision cross sections (CCSs) increase when the charge state increases (Figure 1D), which is often explained by more loosely folded species acquiring more charges. The most obvious for charge state +19 is the presence of several shoulders in the drift time curve, indicative of the presence of different conformers (Figure S2). This was also reported by another research group (using a Synapt G1), where it was interpreted as the consequence of the conformational heterogeneity of PREP.[9] If this were the case, one would expect that the distribution of the protein over the different conformers would change when the ligand is bound. This was not reported, and in our hands, there was but a minor effect of the inhibitor on the distribution over the different conformers (Figure S2). Rather, the single drift time distribution that is apparent in each of the lower charge states (Figure 1C) is indicative of the occurrence of PREP in a limited range of structurally related, folded states, but the highest resolved charge state species +19, and to a lesser extent +18, display a tendency for unfolding, even at the soft acquisition settings used.

Although the measurements with the Synapt G1 instrument did not result in an observable separation of free and ligand-bound PREP, the extracted ion mobility profiles obtained with the Synapt G2 clearly show a comparable symmetrical distribution but with slightly shifted arrival times. The ligand-bound form has a lower mobility for all detected charge states that corresponds to a measured CCS of 4952 Å$^2$ for the charge state +16 (an increase of 45 Å$^2$ or less than 1% of the CCS of free PREP). This can be interpreted as an apparent increase of the overall size after ligand binding compared to the free protein. Although this minute drift in mobility lies within the error range of the Synapt G2 (~40−60 Å$^2$),[4] it was repeatedly observed in samples where free and inhibitor-bound PREP coexisted. The systematic appearance of a ligand-associated shift in mobility and CCS provides evidence for the validity of the observed changes. Similar shifts in mobility were noted when IC-13 binds to Ser554Ala but were not studied in detail because they are not practical for screening ligands. Summarizing, IM-MS data indicate that IC-13 binding to PREP is accompanied by a subtle, but consistent, enlargement of the global structure in the gas phase, while turbidity measurements and small-angle X-ray scattering (SAXS) data

show a decrease in overall dimensions upon ligand binding in solution (Table 1).

The acquired CCS values were cross-validated against the existing structural information, i.e., 11 X-ray structures in the protein structure database,[3,12−16] using the algorithms available to us in 2015. Structures were "cleaned" by removing the solvent and adding missing atoms using a structure editor or modeling program. More extensive manipulations using molecular dynamics, such as energy minimization ("relaxed") or energy minimization in implicit water ("relaxed in water"), had relatively minor effects. The results of the calculations, using different methods, are shown in Figure 2. Accordingly,
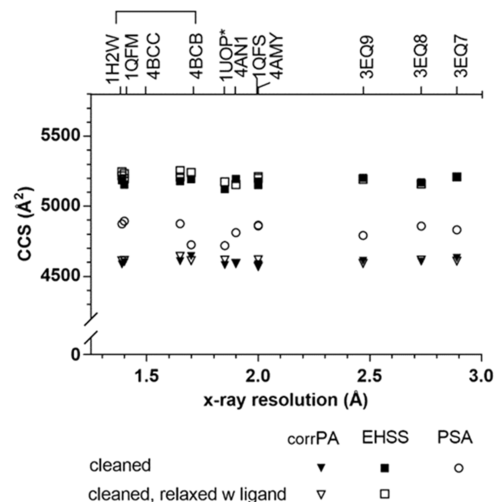


**Figure 2.** CCS calculations using different computational approaches. Eleven porcine PREP structures are identified by their PDB code in the upper axis. PDB 1H2W is a wild-type PREP in the free state at a 1.39 Å resolution, and 4BCB is the complex with IC-13 at a 1.7 Å resolution. PDB entry 1UOP (asterisk) is a structure of Ser554Ala complexed with a peptide substrate at a 1.85 Å resolution. By "cleaned" means the removal of solvent molecules (dehydration) and addition of missing atoms in the coordinates (solid down triangle, solid square, and open circle). Structures minimized in water, with ligands if applicable, are represented by open squares and open down triangles. The abbreviations corrPA, EHSS, and PSAs stand for the corrected Mobcal projection, exact hard-sphere scattering, and projected superposition approximations, respectively.

the experimentally measured CCS for PREP should fall within 4500 Å$^2$ (relaxed in the water corPA value) and 5300 Å$^2$ (relaxed in the water exact hard-sphere scattering (EHSS) value). Experimentally obtained values outside this range are indicative of a structural collapse or unfolding of the protein. The experimental average CCS across the different charge states is 4971 ± 72 Å$^2$, which is well inside this interval, as shown in Figure 1D. For the free wild-type PREP (PDB 1H2W), the predicted range is 4474−5166 Å$^2$, while that of the IC-13-complex (PDB 4BCB) is slightly larger, 4495−5178 Å$^2$ for corPA and EHSS, respectively. Therefore, the existing crystal structures do not provide evidence for ligand binding-induced alterations in the structure of PREP, apart from a very subtle tendency to expand. Hence, to exclude bias from the crystallization process, the coordinates of the closed structure of porcine PREP were modeled to match the open structure of a bacterial PREP (PDB 1YR2), in which the two domains are displaced from each other over an angle of ~30 Å. This corresponded to a 7% increase of the CCS (4803 Å$^2$ [corPA]
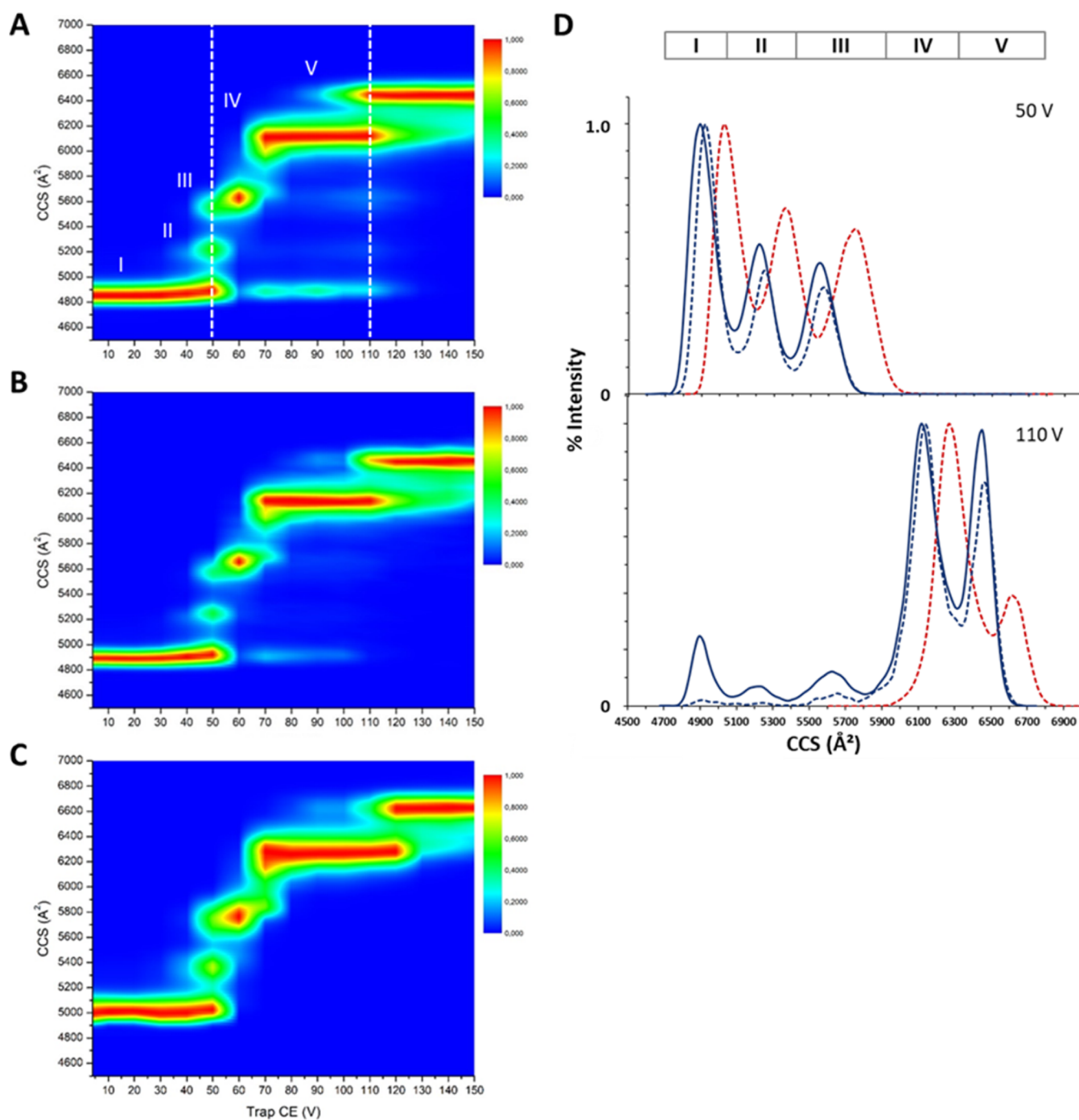
**Figure 3.** CIU of PREP (A), PREP−IC-13 complex (B), and Ser554Ala (C). Unfolding was induced by increasing the voltage of the trap. CIU is accompanied by an initial expansion of the native structure (I) and the formation of 4 additional unfolding intermediates at increasing CE (II−V). The heat maps show the observed CCS plotted against the trap CE voltage, while the contours represent the relative abundance of the intermediates. The dashed lines in panel (A) correlate with the relative position of the folding intermediates in the drift profile of PREP as indicated in panel (D) for Trap CE of 50 and 110 V. Free PREP is indicated with a solid black line, the complex with IC-13 with a dashed gray line, and Ser554Ala with a red dashed line.

and 5511 Å$^2$ [EHSS]) compared with the closed structure. The size of this increase is not unlike the increment in CCS seen between the conformers in the drift time profile of the +19 charge state. However, we do not believe that this result supports a domain opening/closing motion, as has been suggested,[9] but we shall show in the next section that it relates to the CIU pathway of PREP in the gas phase.

**CIU of Free and Ligand-Bound PREP.** Unfolding of PREP in the mass spectrometer was induced by a stepwise increase of the ion activation settings from conditions that preserve the folded structures to values that induce unfolding through an energetic process that increases the internal energy of the molecule in multiple collisions with the inert gas, similar to heating. This can be achieved by increasing the voltage in the sample cone of the electron spray ionization (ESI) source
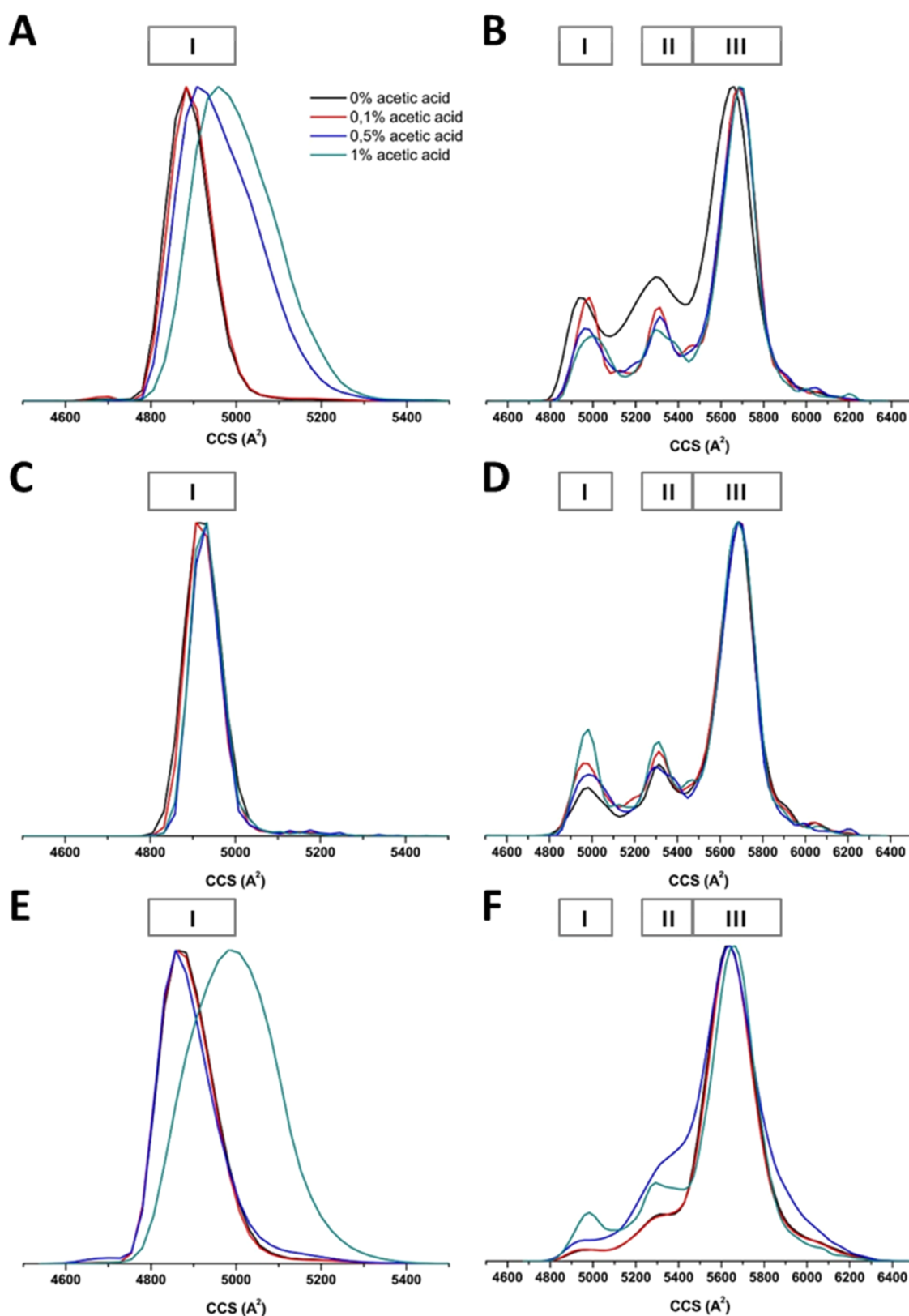
**Figure 4.** Acid denaturation. IM-MS drift profiles for acetic acid-treated PREP (A), the PREP−IC-13 complex (C) and Ser554Ala (E) using nondenaturing ionization/vaporization settings (sample cone 40 V, extractor cone 0.5 V, trap 4 V, transfer cell 0 V, and trap bias voltage 45 V). Panels (B, D, and F) show the corresponding IM-MS drift profiles acquired with 100 V in the sampling cone. Conformers labeled I, II, and III are the same as in Figure 3A.

or by increasing the collision energy (CE) in the trap preceding the ion mobility unit. In both situations, the same

unfolding intermediates are observed. When increasing ion activation, the IM spectra show an extension of the native fold

(from 4946 to 4997 Å$^2$) and the appearance of 2−4 additional distinct ion mobility species at higher drift times (more extended or unfolded species), illustrated in Figure 3 (CIU in the trap). The results of CIU in the sample cone are presented in a more quantitative way in Figures S3 and S4 and as heat plots in Figure S5. As stated above, a domain opening motion would produce a protein similar in size to conformer 2 in the unfolding pathway, but a priori, there is no reason to assume that this is an obligatory step. Similar unfolding patterns were obtained with the IC-13-PREP complex and Ser554Ala (without inhibitor), indicating that, in the gas phase, the intrinsic stabilities of the different species and the unfolding intermediates are very similar.

We consider the unfolding intermediates, observed in the gas phase at different CE settings, as local minima in an unfolding landscape, which can be probed independently of the folding state of the protein at the moment that it is introduced in the ionization/vaporization source. This is most likely a consequence of dehydration, where the removal of water results in highly stable structures of PREP, overruling, e.g., ligand binding-associated stabilization. A key element in this process likely involves the disproportional strengthening of electrostatic forces over the loss of the hydrophobic interactions.

The MS spectra show that IC-13 remains bound to the wild-type PREP during the ion activation experiments. In the crystal structure, this compound forms a covalent bond with the catalytic serine side chain, yet, like other serine protease inhibitors with an electrophilic carbonitrile substituent, it is reversible in solution.[17] Presumably in the context of the PREP active site, both formation and dissociation of the bond are facilitated, establishing an equilibrium in the complex. When the nitrile group is covalently bound to the active serine residue as an imino ether and the active site is disrupted, protonation needed for the reverse reaction does not take place. The proton required for the reverse reaction comes from the catalytic histidine (His680) that is assisted in this process through H-bonding with Asp641. So, from the moment that the structure of the active site is disrupted, whatever inhibitor is bound to the catalytic serine remains attached to the unfolding protein.

The CIU results contrast sharply with the significant effects on the thermal stability in solution after ligand binding and with the observation that Ser554Ala has a higher melting temperature than wild-type PREP (Figure S6). The higher stability of Ser554Ala is not easily understood since it only involves the replacement of a hydroxyl group by a hydrogen atom. However, one may consider that the conformational dynamics of Ser554Ala are altered. Indeed, the substrate-induced conformational change of wild-type PREP involves a movement of the "His-loop" from an outward position toward the active site serine, which results in the assembly of the catalytic triad wherein the Ser554 side chain forms a H-bond with the catalytic His680.[10] Among the inhibitor interfacing residues that are rapidly protected by the inhibitor, as seen in H/D-exchange experiments, is Trp595 of loop B, which goes from an open to closed conformation upon inhibitor binding and shapes the S1 (proline) binding site. Also, the environment of Trp514 is altered upon inhibitor binding.[8] We hypothesized that when the conformational state of the Ser554Ala mutant is different from that of the wild-type PREP, this may affect its fluorescence lifetime. Indeed, tryptophan side chains in PREP have three distinct lifetimes

for the wild type ($t_1 = 8.66 \pm 0.05$ ns, $t_2 = 3.60 \pm 0.03$ ns, $t_3 = 1.15 \pm 0.02$ with $t_m = 3.19 \pm 0.10$ ns) and two for the Ser554Ala mutant ($t_1 = 6.11 \pm 0.03$ ns, $t_2 = 2.07 \pm 0.04$ ns, with $t_m = 3.44 \pm 0.02$ ns).

In Figures 1 and S3, we demonstrated for the first time that IC-13 binds to PREP when the catalytic serine is mutated to alanine, albeit with a lower apparent affinity. Although we could not obtain a quantitative measurement of the binding constant of IC-13 to Ser554Ala by thermal shift, the concentrations required to saturate Ser554Ala for native MS are larger than 10 $\mu$M and this indicates that the loss in affinity due to the mutation is substantial. Inhibitors that lack the carbonitrile substituent (such as IC-9i shown in Figure S1) occupy the same binding site as their covalent counterparts with a $K_i$ in the high nM range.[3,13,17] Therefore, we hypothesize that the inhibitor binding site is conserved in the mutant and, extrapolating to wild-type PREP—that the covalent interaction of the inhibitor with the catalytic serine is not required to induce the conformational change. The crystal structure of Ser554Ala with a bound peptide proves that this mutant can adopt a conformation with all structural elements of the catalytic site intact, except a H-bond between the mutated Ser and His680.[15] Therefore, one assumes that the interaction of the carbonitrile group of IC-13 with the oxy-anion hole (Asn555 main chain and Tyr473 side chain) is maintained.

**Acid Denaturation of PREP in Solution.** To investigate whether CIU bears any resemblance to unfolding in solution, PREP was denatured using 0.1−1% acetic acid (pH < 4), which resulted in a complete loss of the enzymatic activity. Acetic acid is volatile and does not introduce salt ions, which is an advantage in MS measurements. As can be seen in Figure 4A, in soft ionization conditions, acid denaturation is accompanied by a shift toward larger CCS and a broadening of the drift profile, indicative of the presence of several species with different sizes or shapes, corresponding to an expansion of approximately 2.5%. Although enzymatically inactive, the range in CCS of the acid-denatured species indicates that they are not completely unfolded but rather retain a certain amount of structure, as observed for molten globules. In solution, this partial unfolding was prevented by the presence of IC-13 in the samples (Figure 4C) and, as expected, higher concentrations of acetic acid were necessary to denature Ser554Ala (Figure 4E). IM-MS spectra acquired with high CE settings (Figure 4B,D,F) are characterized by three narrow distributions of conformers that appear to be similar in the three experiments. Concluding, the CIU intermediates are formed in the trap regardless of the initial ensemble of conformations in the sample. This means that the key interactions that govern stability in an aqueous solution are fundamentally different from those that determine the unfolding pathway of the dehydrated protein in the gas phase.

**Cysteine Modification.** Cysteines were selected for mutagenesis on the basis of their accessible surface area in the crystal structure of the PREP−inhibitor complex (PDB: 4BCB). Cys25 and Cys532 are exposed on the surface and were mutated to Ala. Cys57, Cys573, and Cys703 are more buried inside the protein and were replaced by hydrophobic side chains that occur in the equivalent positions in other organisms in a multiple sequence alignment. Cys255 is part of the substrate/inhibitor binding site as described before.[18] The Cys255Thr mutant has a reduced enzymatic activity and an altered pH-activity profile. We used a multiple site-directed
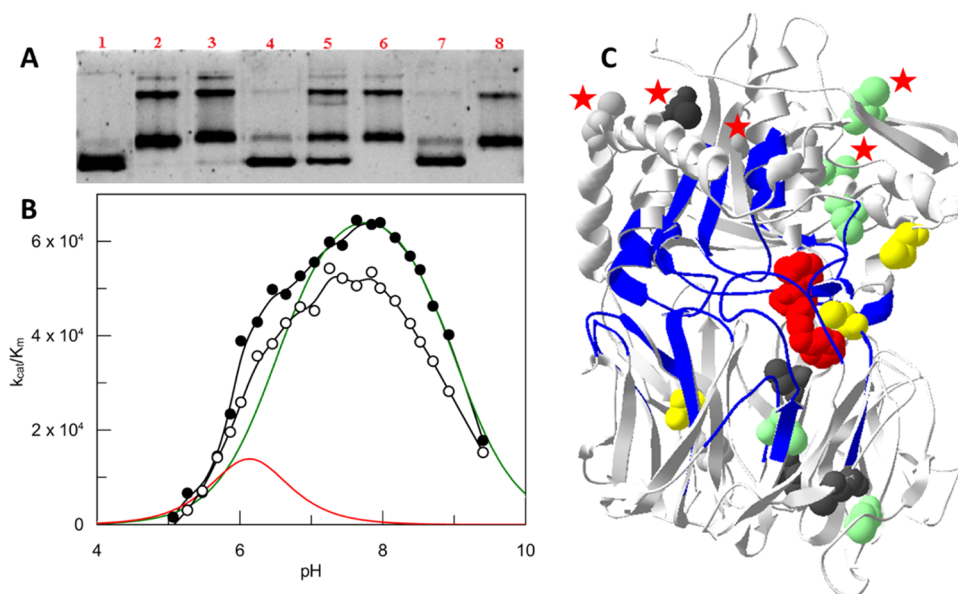
**Figure 5.** PREP cysteine modification. (A) Native polyacrylamide gel with wild type (lanes 1 and 2), 5-Cys (lanes 3 and 4), 5-Cys + Cyst255Thr (lanes 5 and 6), and Cys255Thr (lanes 7 and 8). In the absence of inhibitor (lanes 2, 3, 6, and 8), three bands are resolved migrating at a lower speed than the enzyme−inhibitor complex (lanes 1, 4, 5, and 7). (B) pH-activity profile of the wild type (solid black circle) and the 5-Cys variant (open circle) with 62.5 $\mu$M Z-Gly-Pro-pNA. $k_{cat}/K_m$ is expressed in $M^{-1}$ $s^{-1}$. The pH profile can be deconvoluted in two bell-shaped curves, which is believed to relate to the conformational heterogeneity of the free enzyme.[19] (C) Ribbon representation of the PREP−inhibitor complex (PDB entry 4BCB). The van der Waals surface of IC-13 is shown in red. The sections of the backbone protected by inhibitor in H/D-exchange experiments are shown in blue.[10] Cysteines are shown by their van der Waals surface according to their modification by IAEDANS in the tryptic peptide analysis: yellow, labeled; green, mixture of labeled and free; dark gray, not modified; light gray, not observed. Residues replaced in the 5-Cys variant are indicated by a red star. Of particular interest are Cys78 (yellow) and Cys175 (green) that are buried inside the $\beta$-propeller domain in the complex. The graphic was made with the Swiss-PDB viewer (http://www.expasy.org/spdbv/).

mutagenesis kit with 5 primers on the wild-type sequence and the Cys255Thr mutant. The following variants were picked up and studied: 5-Cys (Cys25Ala−Cys57Ile−C532Ala−Cys573Val−Cys703Val), 5-Cys + Cys255Thr (Cys25Ala−Cys57Ile−C532Ala−Cys573Val−Cys703Val−Cys255Thr). In a preliminary experiment, the wild-type and the Cys mutants were titrated with the colorimetric reagent 5,5′-dithiobis(2-nitrobenzoate). From this experiment, it was apparent that the number of cysteines modified in the wild type is higher than the four expected from the crystal structure. Therefore, some of the cysteines that are buried in the enzyme−inhibitor complex must be exposed in the more flexible free enzyme. In the presence of inhibitor, the number of cysteine modifications is reduced in the wild type and the Cys variants, indicating that other cysteines are involved than the ones that were replaced. In subsequent experiments, the more sensitive fluorescent reagent 5-({2-[(iodoacetyl)amino]ethyl}amino)-naphthalene-1-sulfonic acid (IAEDANS) was used. In the Supporting Information of Tsirigotaki et al.,[10] we already reported that of the 16 cysteines in the wild-type PREP sequence, depending upon the temperature (going from 15 to 40 °C), 8−12 are readily accessible for modification by IAEDANS in the free enzyme under native conditions. In the presence of KYP-2047 (see Figure S1), labeling of only 4 cysteines is observed between 15 and 40 °C. The identity of the cysteines that are accessible to IAEDANS in wild-type PREP and the 5-Cys variant was determined by peptide mapping, monitoring the mass increase of individual tryptic peptides due to IAEDANS (Figure S7). All of the Cys variants and wild-type PREP have a similar thermoinactivation rate at 40 °C (data not shown) and undergo a conformational change upon inhibitor binding as observed by native PAGE (Figure 5A). The 5-Cys variant is

fully active, and its pH-activity profile is unchanged (Figure 5B), whereas the variants containing Cys255Thr were enzymatically impaired similar to the parent mutant Cys255Thr. The results of the cysteine modification experiment are consistent with the results obtained by H/D-exchange experiments,[10] which showed that there are two main areas in the structure that become less flexible upon inhibitor binding: (1) two flexible blades in an otherwise rigid $\beta$-propeller domain and (2) flexible loops in the interdomain interface at the front of PREP (Figure 5C).

Fluorescent labeling by IAEDANS is fairly labor-intensive because the excess label needs to be carefully removed, the protein concentration determined, and the fluorescence calibrated. However, we suggest that a method could be developed and optimized to measure the amount of label attached using (native) mass spectrometry and that such a method could be used with a relatively high throughput for the screening of PREP ligands.

## ■ CONCLUSIONS

Lessons learned from this experience are that the native structure of PREP is not well preserved after desolvation and ionization inside the mass spectrometer and that ligand-induced conformational changes are best studied in solution. Nevertheless, there is reason to believe that free PREP can exist in different conformations in the gas phase within a narrow range of CCS that may not be resolved by the instruments available to us at the time the study was conducted. Furthermore, the experience with PREP reported here emphasizes the importance of CE titration for the judicious and unbiased interpretation of IM-MS results of monomeric proteins.

New insights have emerged concerning the mode of binding of PREP inhibitors with a carbonitrile warhead. IC-13 remains attached to PREP throughout the CIU experiments, indicating that the disruption of the catalytic site stabilizes the covalent bond with the catalytic serine. IC-13 binds to the Ser554Ala mutant, albeit with a reduced affinity, confirming that native mass spectrometry can reveal tight covalent interactions as well as reversible weak binding.

Considering that the catalytically impaired mutant can rescue functions lost in PREP-negative animals, more research must be devoted to elucidating the conformational dynamics and protein—protein interactions of the Ser554Ala protein.

In order to understand the molecular network that lies at the base of the biological effects of PREP inhibitors/ligands, medicinal chemists need to address the conformational dynamics of PREP experimentally. To measure conformational changes, a number of techniques are available that range from simple to quite specialized. Of the techniques introduced in Table 1, there are some that measure size, shape, or dimensions, for example, native PAGE, dynamic light scattering, and SAXS. Between those dynamic light scattering is probably undervalued because, apart from the average hydrodynamic radius, it also measures (poly)dispersity, the size distribution of the different particles in the sample. The relevance for PREP is clear: the free enzyme is heterodisperse, while the enzyme—inhibitor complexes have a narrow size distribution.[6] Other techniques monitor changes in the local environment or accessibility of specific protein segments or side chains. Two-dimensional NMR and hydrogen/deuterium exchange coupled to mass spectrometry brought insights into the parts of PREP where structural changes occur when inhibitors bind, namely, in the loops covering the active site, the interdomain contacts and two flexible β-propeller blades.[7,8,10] The latter techniques are, however, not easily amenable to the screening of a series of compounds. The principle proposed here of using cysteine modification to monitor local structural changes probably has a lower threshold and appears particularly attractive in this case, because PREP has a large number of free cysteines scattered in its primary structure. Using mass spectrometry to detect the labels has an advantage over fluorescence or colorimetric measurements (that yield an average degree of labeling) because it samples individual molecular species (with 0, 1, 2, 3, or more labels attached) and therefore can detect a shift in the distribution of conformations upon ligand binding. Finally, it could be a useful tool for studying the conformational impact of compounds that do not inhibit the catalytic activity of PREP.

## ■ EXPERIMENTAL SECTION

**Materials.** Ammonium acetate solution 7.5 M was obtained from Sigma-Aldrich (Diegem, Belgium), acetic acid from VWR-BDH Prolabo (Leuven, Belgium), and DMSO from Sigma-Aldrich (Diegem, Belgium). Micro Bio-spinTM P-6 gel columns for buffer exchange were from Bio-Rad Laboratories (Temse, Belgium). IAEDANS was obtained from Molecular Probes (Invitrogen, Merelbeke, Belgium). The PREP inhibitors IC-13 and KYP-2047 were synthesized as described.[3,17] All compounds are >95% pure by high-performance liquid chromatography (HPLC) analysis.

**Protein Expression and Purification.** Recombinant porcine PREP (wild type and S554A) was expressed in JM109 *Escherichia coli* cells and purified as described.[19,20] Recombinant human his-tagged PREP was expressed in BL21(DE3) *E. coli* cells and purified as described.[21] In order to increase the compatibility with subsequent

native IM-MS measurements, all steps of the purification were done in 20 mM tris-HCl buffer pH 7.4, supplemented with 1 mM EDTA and 5 mM DTT. The purity of the sample was monitored using PREP activity measurements using Z-Gly-Pro-*p*-nitroanilide (Bachem, Bubendorf, Switzerland), Bradford protein concentration assays, and sodium dodecyl sulfate-PAGE (SDS-PAGE) in combination with fluorescent oreole staining (Bio-Rad Laboratories, Temse, Belgium). The 5-Cys variant was made in the human his-tagged PREP vector using the QuikChange Lightning Multi site-directed mutagenesis kits (Agilent Technologies, Zaventem, Belgium) with the primers listed in Table 2.

### Table 2. Primers Used

| | | |
|---|---|---|
| Cys25Ala | Fwd 5′-ccgtacaggattatcatggtcataaaattg ctgacccttacgcctg-3′ | t73g_g74c |
| Cys57Ile | Fwd 5′-ctgtgccatttcttgagcagattcccatcagagg tttataca-3′ | t169a_g170t |
| Cys532Ala | Fwd 5′-ctgctttgatgactttcaggctgctgctgagtat ctgatc-3′ | t1594g_g1595c |
| Cys573Val | Fwd 5′-atcagagacctgacctctttggtgttgttattgcc caagttg-3′ | t1717g_g1718t |
| Cys703Val | Fwd 5′-gcgttcatcgcgcgggtcctgaacgtcgactg-3′ | t2107g_g2108t |

**Native Ion Mobility Mass Spectrometry.** *Sample Preparation.* Two milligrams/milliliters of protein samples (2 mg/mL) were buffer-exchanged to 200 mM aqueous ammonium acetate (pH 7) in four consecutive steps using gel filtration microbiospin P6 columns. For each measurement, the concentration was adjusted to 5 $\mu$M in 25—200 mM ammonium acetate. When studying ligand binding to PREP, 100 $\mu$M of the IC-13 compound was dissolved in 1% DMSO and added in a 1:10 ratio to the protein sample. In order to allow for the successful formation of protein—ligand complexes, the samples were incubated for at least 15 min before starting the first measurement.

*Instrument Settings.* Most IM-MS experiments were performed on the Synapt G2 HDMS instrument (Waters, Manchester, U.K.) in ion mobility mode, coupled with an automated chip-based nano-electrospray device (Advion TriVersa nanomate; spray voltage 1.75 kV). The instrument was tuned for gentle transfer of intact, native protein, and protein—ligand complexes without causing ion activation before IM separation. For this, the MS and mobility traces for PREP were meticulously evaluated at variable instrumental settings for (i) the absence of ion activation and (ii) coherence between the drift time-based CCS and the calculated CCS values of the reference crystal structure of PREP (pdb 1H2W) using corrected PA (1.14*PA(Mobs/Mexp)2/3),[22] EHSS, and PSA algorithms.

Unless otherwise stated, the sampling and extractor cone voltages, trap and transfer collision energies (CEs), and trap bias voltage were kept at 40, 0.5, 4, 0, and 45 V, respectively. Ion mobility wave height and velocity were optimized to keep tD in the center of the tD range window. Gas flow rates were set at 180 mL/min helium and 90 mL/min IM, and the backing and trap pressures were kept constant at 3 and 0.025 mbar, respectively. Each acquisition contained ~120 s.

*Data Processing and CCS Calibration.* All IM-MS data were analyzed using DriftScopeX and Masslynx 4.1. The extracted drift traces were all processed using 2 × 2 mean smoothing parameters. The measured transit times were converted into collisional cross section by applying a calibration approach with a set of natively folded proteins as external reference standards (BSA, concanavelin A, avidin, and transthyretin).[23,24]

*CCS Calculations.* The CCS values from the available crystallo-graphic data (solvent atoms and atoms related to the crystallization process were excluded) were calculated using the Mobcal projection approximation (PA)[25] exact hard-sphere scattering (EHSS)[26] and projected superposition approximation (PSA)[27−30] programs. The obtained PA values were corrected (corPA) for the scattering phenomena between the ion and buffer gas using the scaling factor CCS = 1.14CCSPA(Mexp/Mpdb)2/3 as described.[22]

*Thermal Shift Assay.* Protein thermal shift assays were done using a real-time polymerase chain reaction (PCR) machine, StepOne Plus

(Applied Biosystems).[31,32] The samples were assayed in 100 mM tris-HCl pH 7.4, 1 mM EDTA, and 3 mM DTT at a final concentration of 6 $\mu$M in 20 $\mu$L. After a 15 min preincubation of the samples in the presence of various concentrations of inhibitor IC-13, the fluorescent dye SYPRO-Orange (Life Technologies, Ghent, Belgium) was added in a 2.2 excess concentration. Temperature was increased by 1 °C/min from 25 to 95 °C, and fluorescence readings were taken at each interval ($E_x/E_m$ 490/530 nm). The data were fitted to the Boltzmann equation using Graphpad Prism6 from which the apparent melting temperature ($T_m$) values were calculated. Samples were measured in quadruplicate, and the experiment was repeated 3 times.

**Cysteine Modification and Peptide Mapping.** PREP (1 mg/mL) was labeled using a 20-fold molar excess of IAEDANS by incubating at 25 °C for 1 h with magnetic stirring in 20 mM tris buffer, pH 7.8. The labeled protein was separated from the free dye by gel chromatography using a PD-10 column. Fluorescence was measured at $E_{xmax}$ 337 nm and $E_{mmax}$ 490 nm in a Tecan Infinite F200 Pro (Tecan, Switzerland) microtiterplate reader. Trypsin Gold, mass spectrometry grade, was purchased from Promega BNL (Leiden, The Netherlands) and used for the digestion of PREP according to the protocol supplied with it. Tryptic peptides were analyzed using standard procedures with a Xevo Triple Quadrupole mass spectrometer (Waters, Manchester, U.K.).

**Enzymatic Activity.** Assay conditions and pH profile measurements are described in ref 21. To determine the pH-activity profiles, initial rates were measured in duplicate (within a single test) and repeated in 3 independent experiments. The within-test variation was around 5%, but the between-test variation was around 20% due to uncertainties in enzyme concentration arising from multiple enzyme dilutions. The general aspect of the curves was not changed between experiments.

**Native Gel Electrophoresis.** 10% polyacrylamide gels were cast in a running buffer without SDS and run according to the instructions provided with the mini Protean system (Bio-Rad Laboratories, Temse, Belgium). Protein bands were visualized with Oreole staining.

**Fluorescence Lifetime.** Time-correlated single-photon counting was used to measure the fluorescence lifetimes of Trp in PREP (200 nM in tris buffer). A Tsunamimode-locked Ti/sapphire laser system (laser source Millenia Pro, diode-pumped CW) was used to create a picosecond pulse laser from Spectra Physics (model 3950C/D). A spectral-physics pulse selector (model 3980) was used to select a frequency at 1.6 MHz, and the frequency tripled to 295 nm by the prism harmonic separator (model GWU23PL). The fluorescence decays were measured with an emission filter of bandwidth 350 ± 5 nm and a magic angle (54.7°) using a PMA 182 photomultiplier from Picoquant. Instrument response function (IRF) was measured by collecting scattered light using a LUDOX TM colloidal silica suspension using an emission filter at 295 nm. The observed time-resolved decay data were deconvoluted with IRF. The fluorescence decay is expressed as a sum of discrete exponentials as follows

$$I(t) = \sum_i \alpha_i \exp(-t/\tau_i)$$

where $i$ is the number of discrete exponentials, and $\alpha_i$ and $\tau_i$ are the amplitudes and lifetimes, respectively. The average lifetimes were calculated by the following equation

$$\tau_m = \sum_i \tau_i \alpha_i / \sum_i \alpha_i$$

The goodness of the fit is judged by the $\chi^2$ and weighted residuals $W(t)$.

## ASSOCIATED CONTENT

### Supporting Information

The Supporting Information is available free of charge at https://pubs.acs.org/doi/10.1021/acs.jmedchem.4c00866.

Structures and half-maximal inhibitory concentration (IC$_{50}$) values for IC-13 and other PREP inhibitors (Figure S1); drift time profile for the +19 charge state of wtPREP and the wtPREP−inhibitor complex (Figure S2); unfolding pattern of +17 charge state species of PREP wt (bound and unbound) and S554A mutant in gas phase at increasing sampling cone settings (Figure S3); quantitative representation of the unfolding data for unbound and bound (*) wtPREP (Figure S4); CIU by increasing the voltage in the sample cone (Figure S5); thermal shift assay (Figure S6); summary of the analysis of tryptic peptides after labeling with IAEDANS (Figure S7); and references (PDF)

## AUTHOR INFORMATION

### Corresponding Authors

**Anne-Marie Lambeir** − *Laboratory of Medical Biochemistry, Department of Pharmaceutical Sciences, University of Antwerp, B-2610 Antwerp, Belgium;* orcid.org/0000-0001-9386-3777; Email: anne-marie.lambeir@uantwerpen.be

**Frank Sobott** − *Laboratory of Biomolecular & Analytical Mass Spectrometry, Department of Chemistry, University of Antwerp, B-2020 Antwerp, Belgium; Astbury Centre for Structural Molecular Biology and School of Molecular and Cellular Biology, University of Leeds, Leeds LS2 9JT, U.K.;* orcid.org/0000-0001-9029-1865; Email: f.sobott@leeds.ac.uk

### Authors

**Roos Van Elzen** − *Laboratory of Medical Biochemistry, Department of Pharmaceutical Sciences, University of Antwerp, B-2610 Antwerp, Belgium;* Present Address: CellCarta, B-2610 Antwerp, Belgium; orcid.org/0009-0000-8215-9178

**Albert Konijnenberg** − *Laboratory of Biomolecular & Analytical Mass Spectrometry, Department of Chemistry, University of Antwerp, B-2020 Antwerp, Belgium;* Present Address: Thermo Fisher Scientific, 5651 GG Eindhoven, The Netherlands

**Pieter Van der Veken** − *Laboratory of Medicinal Chemistry, Department of Pharmaceutical Sciences, University of Antwerp, B-2610 Antwerp, Belgium;* orcid.org/0000-0003-1208-3571

**Matthew J. Edgeworth** − *Waters/Warwick Centre for BioMedical Mass Spectrometry and Proteomics, School of Life Sciences, University of Warwick, Coventry CV4 7AL, U.K.;* Present Address: Crescendo Biologics Ltd., Babraham Research Campus, Cambridge CB22 3AT, U.K.

†**James H. Scrivens** − *Waters/Warwick Centre for BioMedical Mass Spectrometry and Proteomics, School of Life Sciences, University of Warwick, Coventry CV4 7AL, U.K.*

**Vilmos Fülöp** − *School of Life Sciences, University of Warwick, Coventry CV4 7AL, U.K.; Institute of Biochemistry and Medical Chemistry, Medical School, University of Pécs, 7624 Pécs, Hungary*

Complete contact information is available at:
https://pubs.acs.org/10.1021/acs.jmedchem.4c00866

### Notes

## ACKNOWLEDGMENTS

## ABBREVIATIONS USED

IM-MS, ion mobility native mass spectrometry; CCS, collisional cross section; CE, collision energy; CIU, collision-induced unfolding; corrPA, corrected Mobcal projection; EHSS, exact hard-sphere scattering; ESI, electron spray ionization; IAEDANS, 5-({2-[(iodoacetyl)amino]ethyl}-amino)-naphthalene-1-sulfonic acid; IC-13, inhibitor compound 13 described in[3]; PAGE, polyacrylamide gel electrophoresis; PDB, protein structure data bank; PSAs, projected superposition approximations; PREP, prolyl oligopeptidase EC 3.4.21.26; ROS, reactive oxygen species; SAXS, small-angle X-ray scattering

## REFERENCES

(1) Pätsi, H. T.; Kilpeläinen, T. P.; Jumppanen, M.; Uhari-Väänänen, J.; Van Wielendaele, P.; De Lorenzo, F.; Cui, H.; Auno, S.; Saharinen, J.; Seppälä, E.; Sipari, N.; Savinainen, J.; De Meester, I.; Lambeir, A. M.; Lahtela-Kakkonen, M.; Myöhänen, T. T.; Wallén, E. A. A. 5-Aminothiazoles Reveal a New Ligand-Binding Site on Prolyl Oligopeptidase Which is Important for Modulation of Its Protein-Protein Interaction-Derived Functions. *J. Med. Chem.* **2024**, *67*, 5421−5436.

(2) Kilpeläinen, T. P.; Hellinen, L.; Vrijdag, J.; Yan, X.; Svarcbahs, R.; Vellonen, K.-S.; Lambeir, A.-M.; Huttunen, H.; Urtti, A.; Wallen, E. A. A.; Myöhänen, T. T. The effect of prolyl oligopeptidase inhibitors on alpha-synuclein aggregation and autophagy cannot be predicted by their inhibitory efficacy. *Biomed. Pharmacother.* **2020**, *128*, No. 110253.

(3) Van der Veken, P.; Fülöp, V.; Rea, D.; Gerard, M.; Van Elzen, R.; Joossens, J.; Cheng, J. D.; Baekelandt, V.; De Meester, I.; Lambeir, A. M.; Augustyns, K. P2-substituted N-acylprolylpyrrolidine inhibitors of prolyl oligopeptidase: biochemical evaluation, binding mode determination, and assessment in a cellular model of synucleinopathy. *J. Med. Chem.* **2012**, *55*, 9856−9867.

(4) Konijnenberg, A.; Butterer, A.; Sobott, F. Native ion mobility-mass spectrometry and related methods in structural biology. *Biochim. Biophys. Acta, Proteins Proteomics* **2013**, *1834*, 1239−1256.

(5) Niu, S.; Rabuck, J. N.; Ruotolo, B. T. Ion mobility-mass spectrometry of intact protein-ligand complexes for pharmaceutical drug discovery and development. *Curr. Opin. Chem. Biol.* **2013**, *17*, 809−817.

(6) Szeltner, Z.; Juhász, T.; Szamosi, I.; Rea, D.; Fülöp, V.; Módos, K.; Juliano, L.; Polgár, L. The loops facing the active site of prolyl oligopeptidase are crucial components in substrate gating and specificity. *Biochim. Biophys. Acta, Proteins Proteomics* **2013**, *1834*, 98−111.

(7) López, A.; Herranz-Trillo, F.; Kotev, M.; Gairí, M.; Guallar, V.; Bernadó, P.; Millet, O.; Tarragó, T.; Giralt, E. Active-Site-Directed Inhibitors of Prolyl Oligopeptidase Abolish Its Conformational Dynamics. *ChemBioBhem* **2016**, *17*, 913−917.

(8) Tarragó, T.; Claasen, B.; Kichik, N.; Rodriguez-Mias, R. A.; Gairí, M.; Giralt, E. A Cost-Effective Labeling Strategy for the NMR Study of Large Proteins: Selective 15N-Labeling of the Tryptophan Side Chains of Prolyl Oligopeptidase. *ChemBioChem* **2009**, *10*, 2736−2739.

(9) López, A.; Vilaseca, M.; Madurga, S.; Varese, M.; Tarragó, T.; Giralt, E. Analyzing slowly exchanging protein conformations by ion mobility mass spectrometry: study of the dynamic equilibrium of prolyl oligopeptidase. *J. Mass Spectrom.* **2016**, *51*, 504−511.

(10) Tsirigotaki, A.; Van Elzen, R.; Van Der Veken, P.; Lambeir, A. M.; Economou, A. Dynamics and ligand-induced conformational changes in human prolyl oligopeptidase analyzed by hydrogen/deuterium exchange mass spectrometry. *Sci. Rep.* **2017**, *7*, No. 2456.

(11) Di Daniel, E.; Glover, C. P.; Grot, E.; Chan, M. K.; Sanderson, T. H.; White, J. H.; Ellis, C. L.; Gallagher, K. T.; Uney, J.; Thomas, J.; Maycox, P. R.; Mudge, A. W. Prolyl oligopeptidase binds to GAP-43 and functions without its peptidase activity. *Mol. Cell. Neurosci.* **2009**, *41*, 373−382.

(12) Fulop, V.; Bocskei, Z.; Polgar, L. Prolyl oligopeptidase: an unusual beta-propeller domain regulates proteolysis. *Cell* **1998**, *94*, 161−170.

(13) Kaszuba, K.; Rog, T.; Danne, R.; Canning, P.; Fulop, V.; Juhasz, T.; Szeltner, Z.; St Pierre, J.-F.; Garcia-Horsman, A.; Mannisto, P. T.; Karttunen, M.; Hokkanen, J.; Bunker, A. Molecular dynamics, crystallography and mutagenesis studies on the substrate gating mechanism of prolyl oligopeptidase. *Biochimie* **2012**, *94*, 1398−1411.

(14) Kánai, K.; Aranyi, P.; Bocskei, Z.; Ferenczy, G.; Harmat, V.; Simon, K.; Batori, S.; Naray-Szabo, G.; Hermecz, I. Prolyl Oligopeptidase Inhibition by N-Acyl-pro-pyrrolidine-type Molecules. *J. Med. Chem.* **2008**, *51*, 7514−7522.

(15) Fülöp, V.; Szeltner, Z.; Renner, V.; Polgár, L. Structures of prolyl oligopeptidase substrate/inhibitor complexes. Use of inhibitor binding for titration of the catalytic histidine residue. *J. Biol. Chem.* **2001**, *276*, 1262−1266.

(16) Szeltner, Z.; Rea, D.; Renner, V.; Juliano, L.; Fülöp, V.; Polgár, L. Electrostatic environment at the active site of prolyl oligopeptidase is highly influential during substrate binding. *J. Biol. Chem.* **2003**, *278*, 48786−48793.

(17) Venäläinen, J. I.; Garcia-Horsman, J. A.; Forsberg, M. M.; Jalkanen, A.; Wallen, E. A.; Jarho, E. M.; Christiaans, J. A.; Gynther, J.; Mannisto, P. T. Binding kinetics and duration of in vivo action of novel prolyl oligopeptidase inhibitors. *Biochem. Pharmacol.* **2006**, *71*, 683−692.

(18) Szeltner, Z.; Renner, V.; Polgar, L. The Noncatalytic β-Propeller Domain of Prolyl Oligopeptidase Enhances the Catalytic Capability of the Peptidase Domain. *J. Biol. Chem.* **2000**, *275*, 15000−15005.

(19) Szeltner, Z.; Renner, V.; Polgar, L. Substrate- and pH-dependent contribution of oxyanion binding site to the catalysis of prolyl oligopeptidase, a paradigm of the serine oligopeptidase family. *Protein Sci.* **2000**, *9*, 353−360.

(20) Brandt, I.; Gérard, M.; Sergeant, K.; Devreese, B.; Baekelandt, V.; Augustyns, K.; Scharpé, S.; Engelborghs, Y.; Lambeir, A. M. Prolyl oligopeptidase stimulates the aggregation of alpha-synuclein. *Peptides* **2008**, *29*, 1472−1478.

(21) Van Elzen, R.; Schoenmakers, E.; Brandt, I.; Van Der Veken, P.; Lambeir, A. M. Ligand-induced conformational changes in prolyl oligopeptidase: a kinetic approach. *Protein Eng., Des. Sel.* **2017**, *30*, 217−224.

(22) Hall, Z.; Politis, A.; Bush, M. F.; Smith, L. J.; Robinson, C. V. Charge-state dependent compaction and dissociation of protein complexes: insights from ion mobility and molecular dynamics. *J. Am. Chem. Soc.* **2012**, *134*, 3429−3438.

(23) Bush, M. F.; Hall, Z.; Giles, K.; Hoyes, J.; Robinson, C. V.; Ruotolo, B. T. Collision cross sections of proteins and their complexes: a calibration framework and database for gas-phase structural biology. *Anal. Chem.* **2010**, *82*, 9557−9565.

(24) Ruotolo, B. T.; Benesch, J. L.; Sandercock, A. M.; Hyung, S. J.; Robinson, C. V. Ion mobility-mass spectrometry analysis of large protein complexes. *Nat. Protoc.* **2008**, *3*, 1139−1152.

(25) Wyttenbach, T.; von Helden, G.; Batka, J. J.; Carlat, D.; Bowers, M. T. Effect of the long-range potential on ion mobility measurements. *J. Am. Soc. Mass Spectrom.* **1997**, *8*, 275−282.

(26) Shvartsburg, A. A.; Jarrold, M. F. An exact hard-spheres scattering model for the mobilities of polyatomic ions. *Chem. Phys. Lett.* **1996**, *261*, 86−91.

(27) Bleiholder, C.; Wyttenbach, T.; Bowers, M. T. A novel projection approximation algorithm for the fast and accurate computation of molecular collision cross sections (I) Method. *Int. J. Mass Spectrom.* **2011**, *308*, 1−10.

(28) Bleiholder, C.; Contreras, S.; Bowers, M. T. A novel projection approximation algorithm for the fast and accurate computation of molecular collision cross sections (IV). Application to polypeptides. *Int. J. Mass Spectrom.* **2013**, *354-355*, 275−280.

(29) Wyttenbach, T.; Bleiholder, C.; Bowers, M. T. Factors Contributing to the Collision Cross Section of Polyatomic Ions in the Kilodalton to Giga dalton Range: Application to Ion Mobility Measurements. *Anal. Chem.* **2013**, *85*, 2191−2199.

(30) Bleiholder, C.; Contreras, S.; Do, T. D.; Bowers, M. T. A Novel Projection Approximation Algorithm for the Fast and Accurate Computation of Molecular Collision Cross Sections (II). Model Parameterization and Definition of Empirical Shape Factors for Proteins. *Int. J. Mass Spectrom.* **2013**, *345−347*, 89−96.

(31) Ericsson, U. B.; Hallberg, B. M.; Detitta, G. T.; Dekker, N.; Nordlund, P. Thermofluor-based high-throughput stability optimization of proteins for structural studies. *Anal. Biochem.* **2006**, *357*, 289−298.

(32) Vedadi, M.; Niesen, F. H.; Allali-Hassani, A.; Edwards, A. M.; et al. Chemical screening methods to identify ligands that promote protein stability, protein crystallization, and structure determination. *Proc. Natl. Acad. Sci. U.S.A.* **2006**, *103*, 15835−15840.

## ■ NOTE ADDED AFTER ASAP PUBLICATION

The author information was incomplete when this paper was published on May 24, 2024. The list of authors, Author Information, and Acknowledgments were updated and the paper reposted on June 13, 2024.